Synchrony and idiosyncrasy in the gut microbiome of wild baboons

Authors: Johannes R. Björk[1*], Mauna R. Dasari[1], Kim Roche[2], Laura Grieneisen[3], Trevor J. Gould[3], Jean-Christophe Grenier[4,5], Vania Yotova[4], Neil Gottel[6], David Jansen[1], Laurence R. Gesquiere[7], Jacob B. Gordon[7], Niki H. Learn[8], Tim L. Wango[9,10], Raphael S. Mututua[9], J. Kinyua Warutere[9], Long'ida Siodi[9], Sayan Mukherjee[2], Luis B. Barreiro[11], Susan C. Alberts[7,12,13], Jack A. Gilbert[6], Jenny Tung[7,12,13,14], Ran Blekhman[3,15], Elizabeth A. Archie[1*]

Affiliations:

[1] Department of Biological Sciences, University of Notre Dame, Notre Dame, IN 46556, USA

[2] Program in Computational Biology and Bioinformatics, Duke University, Durham, NC 27708, USA

[3] Department of Genetics, Cell Biology, and Development, University of Minnesota, Minneapolis, MN 55455, USA

[4] Department of Genetics, CHU Sainte Justine Research Center, Montréal, QC, H3T1C5, Canada.

[5] Research Center, Montreal Heart Institute, Montréal, Quebec H1T 1C8, Canada

[6] Department of Pediatrics and the Scripps Institution of Oceanography, University of California, San Diego, San Diego, CA 92093, USA

[7] Department of Biology, Duke University, Durham, NC 27708, USA

[8] Department of Ecology and Evolutionary Biology, Princeton University, Princeton, NJ 08544, USA

[9] Amboseli Baboon Research Project, Amboseli National Park, Kenya

[10] The Department of Veterinary Anatomy and Animal Physiology, University of Nairobi, Kenya

[11] Department of Medicine, Section of Genetic Medicine, University of Chicago, Chicago, IL 60637, USA

[12] Department of Evolutionary Anthropology, Duke University, Durham, NC 27708, USA

[13] Duke University Population Research Institute, Duke University, Durham, NC 27708, USA

[14] Canadian Institute for Advanced Research, Toronto, Ontario M5G 1M1, Canada

[15] Department of Ecology, Evolution, and Behavior, University of Minnesota, Minneapolis, MN 55455, USA

* Correspondence to: bjork.johannes@gmail.com; earchie@nd.edu

Abstract: Human gut microbial dynamics are highly individualized, making it challenging to link microbiota to health and to design universal microbiome therapies. This individuality is typically attributed to variation in host genetics, diets, environments, and medications, but it could also emerge from fundamental ecological forces that shape microbiota more generally. Here we leverage extensive gut microbial time series from wild baboons—hosts who experience little interindividual dietary and environmental heterogeneity—to test whether gut microbial dynamics are synchronized across hosts or largely idiosyncratic. Despite their shared lifestyles, baboon microbiome dynamics were only weakly synchronized. The strongest synchrony occurred among baboons living in the same social group, likely because group members range over the same habitat and simultaneously encounter the same sources of food and water. However, this synchrony was modest compared to each host's personalized dynamics. Indeed, host-specific factors, especially host identity, explained 10 times the deviance in longitudinal microbial dynamics, compared to factors shared across hosts. These results contribute to mounting evidence that highly idiosyncratic gut microbiomes are not an artifact of modern human environments, and that synchronizing forces in the gut microbiome (e.g., shared environments, diets, and microbial dispersal) are often not strong enough to overwhelm drivers of microbiome personalization, including host genetics, priority effects, horizontal gene transfer, and functional redundancy.

Introduction

Mammalian gut microbiotas are highly complex, dynamic ecosystems. From these dynamics emerge a set of life-sustaining services for hosts, which help them digest food, process toxins, and resist invading pathogens. Despite their importance, our understanding of how gut microbial communities change over months and years within hosts, especially the collective dynamics of microbiotas from hosts living in the same population, is relatively poor[1, 2]. This gap exists in part because we lack time series data that track gut microbiota longitudinally across many hosts living together in the same population. As a result, it has been difficult to answer key questions. For example, when host populations encounter shifting environments and resources, does each host's microbiota respond similarly—i.e., in synchrony—or idiosyncratically to these changes? Further, what factors predict synchronized versus idiosyncratic microbiota?

Answering these questions is important because synchronized gut microbial communities, if and when they occur[1], could help explain shared microbiota-associated traits in host populations, such as patterns of disease susceptibility[3, 4]. A high degree of microbiome synchrony could also be good news for researchers working to predict microbial dynamics because it would suggest that similar ecological principles govern changes in microbial composition across hosts[5]. There is also theoretical justification to expect some degree of coordinated dynamics, as host populations and their microbiotas can be considered a 'microbiome metacommunity' (see e.g.,[6, 7, 8, 9]). Metacommunity theory predicts that synchrony will arise across microbiotas if their hosts experience similar environmental conditions and/or high rates of microbial dispersal between hosts[10, 11]. In support, fruit bats living in the same colony exhibit coordinated fur microbiota dynamics, and shared environments and microbial dispersal are both implicated in this synchrony[1].

However, even in the presence of such synchronizing forces, there are many reasons to expect that hosts in a microbiome metacommunity will exhibit idiosyncratic (i.e., individualized) microbial compositions and dynamics. First, idiosyncratic dynamics are expected when the same microbes in different hosts respond in different ways to environmental fluctuations, chance events, and/or interactions with other microbes[12, 13, 14, 15]. These forces are likely to be important in gut microbiota where priority effects, functional redundancy, and horizontal gene flow can cause the same microbial taxon to perform different functions, play different ecological roles, and exhibit different environmental responses in different hosts (or cause different microbial taxa to play the same role in different hosts)[16, 17, 18, 19]. Second, several cross-sectional studies, in both humans and animals, find that individual hosts exhibit distinctive gut microbiota, and host identity explains a large fraction of population-wide microbiome taxonomic variation[1, 20, 21, 22, 23, 24, 25]. These results suggest that longitudinal gut microbial changes are also likely to be asynchronous across hosts. Indeed, some longitudinal studies in humans and animals find personalized gut microbial dynamics[1, 24, 26, 27, 28], which are usually attributed to interpersonal differences in diet, medications, and lifestyle[27, 29, 30, 31]. If these explanations are correct, then observed idiosyncrasy in microbiome dynamics may be simply explained by a lack of shared environmental drivers rather than distinct microbiome responses to shared environments (but see [27]). In contrast, if personalized dynamics persist even when hosts share the same environment, then (i) host-specific dynamics may not be solely attributable to interpersonal differences in

93 lifestyles; (ii) predicting the dynamics of microbial taxa in individual hosts may prove difficult;
94 and (iii) microbiome interventions that rely on manipulating taxa may face challenges beyond
95 heterogeneity in lifestyles, and instead may be related to conserved ecological principles that
96 govern the gut microbiome.

97

98 **Data and methods**

99 Here we test the degree to which gut microbial taxonomic composition and dynamics, as
100 measured via 16S rRNA gene sequencing, are synchronized versus idiosyncratic in wild baboon
101 hosts living in the Amboseli ecosystem in Kenya[32]. Baboons are terrestrial primates that live in
102 stable social groups, typically with 20 to 130 members. The 600 baboons in our data set lived in
103 12 social groups over a 14-year span (April 2000 to September 2013; 5 original groups and 7
104 groups that were fission/fusion products from these original groups; **Fig. 1A**). The baboons were
105 members of the well-studied Amboseli baboon population[32], which has been followed by the
106 Amboseli Baboon Research Project since 1971. This project collected detailed longitudinal data
107 on rainfall and temperature; social group membership, ranging patterns and diet; and host traits
108 such as age, sex, social relationships, and dominance rank (see Supplementary Materials).

109 Like many natural animal populations, the Amboseli baboons experience shared diets,
110 environments, and opportunities for between-host microbial dispersal that have the potential to
111 drive microbiota synchrony across hosts. Because baboons are not territorial, all 12 baboon
112 social groups used an overlapping ~60 km^2 range (**Fig. 1B**; **video S1**;[33]). Hence all animals were
113 exposed to similar microbes from the environment and shared seasonal changes in rainfall and
114 temperature[33, 34, 35]. The Amboseli ecosystem is a semi-arid savanna with a 5-month long dry
115 season spanning June to October, during which very little rain falls. The remaining 7 months
116 (November to May) constitute the wet season, which is characterized by highly variable rainfall
117 (**Fig. 1C**; mean annual rainfall between 2000 and 2013 was 319 mm; range = 140 mm to 559
118 mm). These seasonal shifts in climate drive a rotating set of foods consumed by the baboons:
119 during the dry season the baboons rely largely on grass corms, shifting to growing grass blades
120 and grass seed heads in the wet season (**Fig. 1D**). Within baboon social groups, diets and
121 environments are especially congruent because group members travel together in a coordinated
122 fashion across the landscape, encountering and consuming resources and feeding on the same

123 seasonally available foods at the same time[33, 36, 37, 38, 39, 40]. Group members also groom each
124 other, combing through each other's fur and placing some items in their mouths, which may
125 contribute to host-to-host microbial transmission[41]. Finally, at the level of individual hosts, host
126 genetic variation has a consistent, albeit modest, effect on gut microbial composition in this
127 population[33]. Other host-specific traits, like age, sex, and social status, also lead some individuals
128 to share aspects of their behavior, immune profiles, and physiology, which could also lead to
129 more congruent microbial dynamics.

130 A key advance in our study is longitudinal sampling of gut microbial composition from
131 fecal samples collected from hundreds of known baboons throughout their lives (**Fig. 1A**). Such
132 dense, long-term, longitudinal microbiota sampling is difficult to achieve in many animals,
133 including humans. The 17,265 fecal samples in our study were collected from baboons who
134 ranged in age from 7.4 months to 27.7 years, spanning these animals' natural lifespans (**fig.**
135 **S1A**). Each baboon was sampled a median of 19 times, and 124 baboons were sampled at least
136 50 times (**fig. S1B**). On average, these samples spanned 4.3 years of a baboon's life (range = 4
137 days to 13.2 years; **fig. S1C**), with a median of 35 days between consecutive samples (**fig. S1D**).

138 A large majority of the microbiota data we use here were published in Grieneisen et al.[33],
139 but we include data from 1,031 additional samples that were generated at the same time using the
140 same methods (they were not included in the heritability analysis of Grieneisen et al.[33] because
141 we lack pedigree information for these hosts). Briefly, we generated 896,911,162 sequencing
142 reads (mean = 51,913.6 reads per sample; range = 1021 - 477,241, **fig. S1E**). We retained
143 microbial amplicon sequence variants (ASVs) with a minimum of 3 reads per sample. DNA
144 concentration and ASV diversity were not predicted by time since sample collection (**fig. S1G,**
145 **S1H**). To allow us to compare the dynamics of individual taxa in different hosts, we focused on
146 taxa that were common across hosts, retaining only those found in at least 20% of samples. This
147 filtering resulting in 341 ASVs (mean = 162 ASVs per sample; range = 19 - 311 ASVs; **fig S1F;**
148 **table S1**). While this filtering was somewhat stringent, it captured 92% of the reads and many of
149 the same compositional properties of the data set when filtered to 5% prevalence (**fig. S2**). As is
150 typical for wild microbiota, 22.9% of the 341 ASVs could not be assigned to a known family (78
151 of 341), and 5.5% of ASVs could not be assigned to a known phylum (19 of 341; **table S1**). To
152 address the compositional nature of our data, read counts were centered log-ratio (clr)
153 transformed independently in each sample (including independent transforms for samples from

the same individual), prior to all analyses[42, 43]. Therefore, our results must be considered with respect to the chosen reference frame, which in this case is the geometric mean of taxon abundances in each sample, or the abundance of a sample's 'average microbe'.

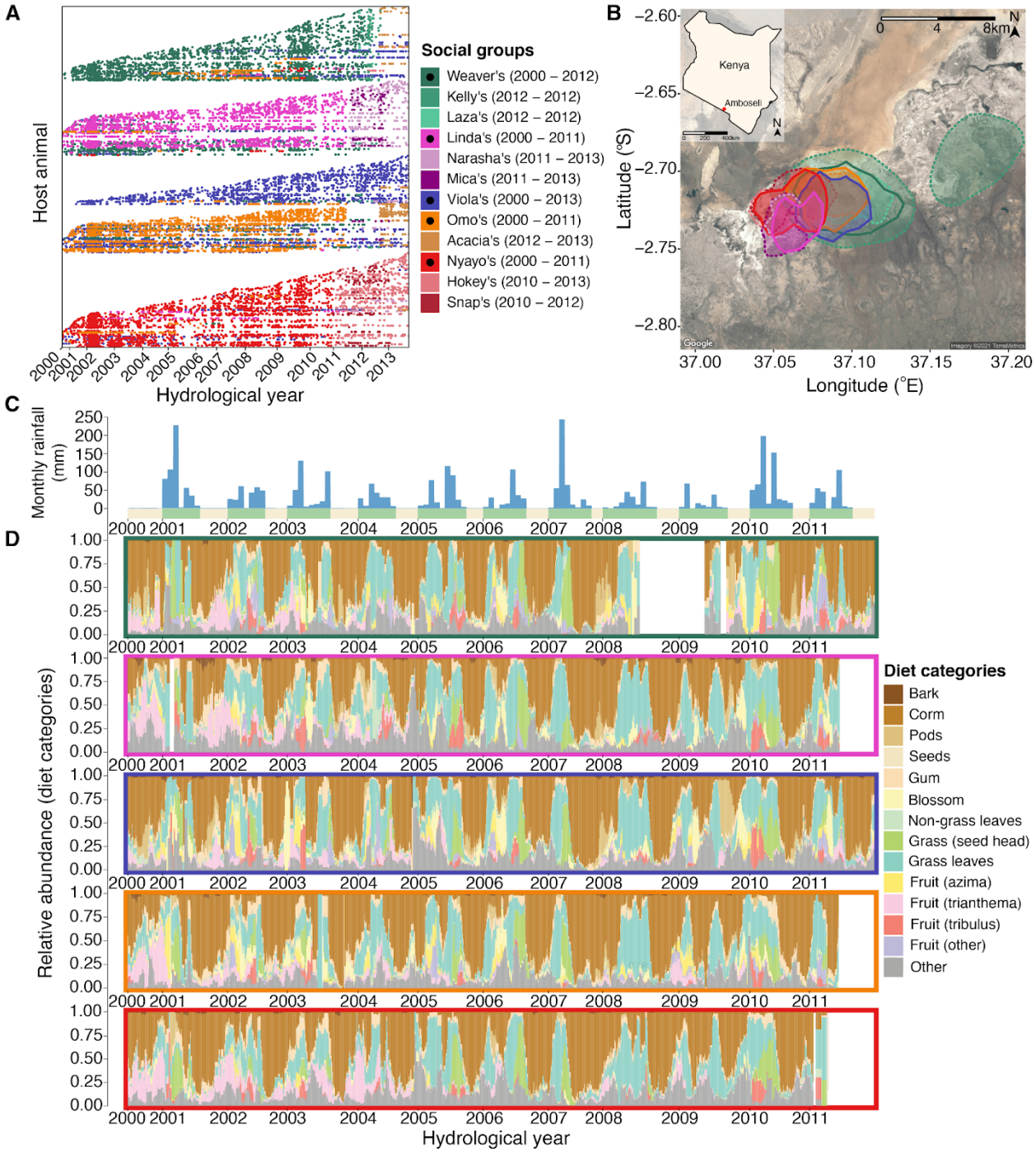

Fig. 1. Baboons in Amboseli experience shared environments at multiple scales. (A) Our microbiota time series consisted of 17,265 16S rRNA gene sequencing gut microbial profiles. Each point represents a microbiota sample, plotted by the date it was collected (x-axis). Each

row (y-axis) corresponds to a unique individual host. Samples were collected from 600 wild baboons living in 5 original social groups (indicated by dark colors marked with black dots in the legend) and 7 groups that fissioned/fused from these original groups (no black dots). **(B)** All baboon groups ranged over a shared ~60 km^2 area, and the social groups had largely overlapping home ranges. Ranges are shown as 90% kernel densities over the sampling period specific to each group; 5 original social groups are shown with solid borders, fission and fusion products with dashed borders. **(C)** Monthly rainfall amounts (blue bars, in mm) with yellow and green stripes along the x-axis representing dry and wet seasons, with the width of the green stripes reflecting the number of months within the focal year that had at least 1 mm rainfall. **(D)** Temporal shifts in diet from the years 2000 – 2013, shown as the relative abundance of diet components in the 5 original social groups over 30-day sliding windows prior to each sample collection date. Colors correspond to the 13 most common food types, while the grey bars correspond to other or unknown food types. Colored boxes around each panel reflect each of the 5 original, most extensively sampled social groups (colors as in plots A and B). The white bars indicate time periods where no diet data were collected.

To test whether shared environmental conditions and host traits lead to similar gut microbial compositions and synchronized dynamics across the microbiome metacommunity, we used three main approaches (see Supplementary Materials for details of all analyses). First, we characterized patterns of temporal autocorrelation in ASV-level Aitchison similarity within and between hosts over time. Our expectation was that, if hosts or social groups exhibit idiosyncratic composition and dynamics, then samples collected close in time from the same baboon, or from baboons in the same group, should be much more similar than they are to samples collected from different baboons living in different groups. Alternatively, if gut microbial dynamics are strongly synchronized, then samples collected close in time across the metacommunity should be compositionally similar, and samples collected from the same host should not be substantially more similar than samples from different baboons. These analyses were run in R (v 4.0.2; [44]) using custom-written functions (code and analyzed data are available on GitHub/OSF; see Data Statement).

Second, to test whether dispersal limitation could explain microbiome idiosyncrasy, we estimated metacommunity-wide microbial migration probabilities in each season and year using the Sloan Neutral Community Model for Prokaryotes[45, 46]. This model assumes that each local community, defined as the ASV-level microbial composition of a single host in a given season-year combination, is the outcome of stochastic population dynamics and microbial immigration

195 from other hosts in the microbiome metacommunity (i.e., other local communities). Briefly, local
196 communities have a constant size *N*, and individual microbes within each local community die at
197 a constant rate. These deaths create vacancies that can be occupied, either by individuals
198 immigrating from the microbiome metacommunity (with probability *m*), or by daughter cells
199 from any taxon within the local community (i.e., from reproduction within the same host, with
200 probability 1-*m*). Taxa that are common in the metacommunity have a higher chance of
201 occupying vacancies than rare taxa. Without immigration from the microbiome metacommunity,
202 ecological drift leads each host's microbial diversity to reduce to a single taxon. Thus, the
203 migration probability, *m*, represents the metacommunity-wide probability that any taxon,
204 randomly lost from a given host/local community, will be replaced by dispersal from the
205 microbiome metacommunity, as opposed to reproduction within hosts[45, 46]. Following Burns et
206 al.[47], *m* can be interpreted as a measure of dispersal limitation, such that low migration
207 probabilities signify high dispersal limitation. We estimated season and hydrological year-
208 specific values for *m* by defining the microbiome metacommunity as either the hosts' social
209 group or the whole host population. We fit neutral models using nonlinear least-squares
210 regression as implemented in the R package tyRa[48].

211 Third, to quantify the relative magnitude of idiosyncratic versus synchronized dynamics
212 for community metrics and common families and phyla, we used generalized additive models
213 (GAMs) to capture the non-linear, longitudinal dynamics of 52 features, including the first three
214 principal components of ASV-level composition, three indices of alpha diversity (ASV richness,
215 the exponent of ASV-level Shannon's H, and the inverse Simpson index for ASVs, as computed
216 by the function reyni from the R package vegan[49]), and the clr-transformed abundances of 12
217 phyla and 34 families present in >20% of samples. We analyzed phyla and families (as opposed
218 to genera or ASVs) because phyla and families are highly prevalent across samples (mean
219 prevalence = 85.6% for the 12 phyla and 73.7% for the 34 families), offering excellent power to
220 compare their dynamics between different baboons. We note, however, that phyla and families
221 might be expected to exhibit stronger synchrony than lower-level taxa because, compared to
222 species or strains, the dynamics of families and phyla reflect multiple microbial processes and
223 interactions, which are expected to buffer them against large fluctuations in abundance. Further,
224 the processes and interactions that a given phylum or family collectively encompasses may be

225 more consistent across hosts than those carried out by an individual species or strain (although
226 this consistency will vary depending on the phylum, family, or process in question[18, 50]).
227 Our GAMs allowed us to calculate the percent deviance in each feature's dynamics
228 attributable to factors that could contribute to synchronized dynamics at different scales (percent
229 deviance is a measure of goodness-of-fit for nonlinear models and is analogous to the unadjusted
230 R^2 for linear models). We considered deviance explained by factors at three scales: those
231 experienced by the whole host population (e.g., rainfall and temperature), those differentiated by
232 social groups (e.g., group identity, group home range location, and diet), and those differentiated
233 at the level of individual hosts (e.g., host identity, sex, age, and social dominance rank; see below
234 for complete model structures). If microbiome community dynamics are largely idiosyncratic,
235 then population- and group-level factors will not explain considerable deviance in microbiota
236 change over time, and instead, a large fraction of the deviance will be attributable to host
237 identity, controlling for shared environments, behaviors, and traits. Alternatively, if shared
238 environments and behaviors across the population and within social groups synchronize gut
239 microbiota, then population- and group-level factors should explain substantial deviance in
240 community dynamics. To ensure sufficiently dense sampling for identifying host- and group-
241 level dynamics, all three GAMs were run on a subset of the full data set, consisting of 4,277 16S
242 rRNA gene sequencing profiles from the 56 best-sampled baboons living in the 5 social groups
243 sampled the longest (between 2002 and 2010; median = 72.5 samples per host; minimum = 48
244 samples; maximum = 164 samples; **fig. S3**). GAMs were fit using the R package mgcv[51, 52, 53].
245 Notably, the GAM approach allows us to identify the percent deviance attributable to
246 host identity, but does not identify the specific characteristics that account for host identity
247 effects. Genetic effects are a likely candidate, as previous analyses demonstrate that taxon
248 abundance and summaries of gut microbiome position are lowly to moderately heritable in this
249 population[33]. To evaluate this possibility, we performed a *post hoc* analysis of the relationship
250 between the deviance explained in the GAMs for each microbial taxon and the heritability of that
251 taxon's relative abundance[33]. If host effects on microbiome dynamics are in part explained by
252 host genotype, we predicted that taxon heritability should be positively correlated with deviance
253 explained at the host level (i.e., model P+G+H), but not at the group or population level (i.e.,
254 model P and model P+G).
255

256 **Results and Discussion**

257 **Baboon gut microbiota exhibit cyclical shifts in community composition across seasons and**
258 **years**

259 We began by visualizing annual and inter-annual fluctuations across all 600 hosts (17,265
260 samples) over the 14-year span of the data. Consistent with prior research on primates[54, 55, 56], we
261 found population-wide, cyclical shifts in microbiome community composition across seasons
262 and years (**Fig. 2**). This wet-dry seasonal cyclicity was primarily observable in the first principal
263 component (PC1) of a principal component analysis (PCA) of clr-transformed ASV read counts
264 (**Fig. 2A, 2B**; **fig. S4-S6**; PC1 explains 16.5% of the variance in microbiome community
265 composition). PC1 exhibited its lowest values during the dry season, and highest values during
266 the wet season, mirroring monthly rainfall (**Fig. 2B; fig. S6**). Consistent with these annual,
267 seasonal fluctuations, periodicity for PC1, calculated as the mean distance between major peaks,
268 was 374 days. PC1 was also linked to annual rainfall across years, exhibiting especially low
269 values throughout 2008 and 2009, which corresponded to the worst continuous drought in the
270 Amboseli ecosystem in 50 years (**Fig. 2A, 2B**). We also observed small, but statistically
271 significant seasonal differences in PC2 and PC3 (8.4% and 3.7% of variation in community
272 composition; **Fig. 2C**; **fig. S4-S6**) and in measures of alpha diversity (**Fig. 2C**; **fig. S6, S7**), as
273 has been reported in other ecosystems[57]. Together, these seasonal changes are probably caused
274 by seasonal shifts in plant phenology and its effects on diet (**Fig. 1D**), as well as the effects of
275 rainfall and other weather variables on bacterial exposures from the abiotic environment (e.g.,
276 soil communities and sources of drinking water).

277 In terms of individual microbiome taxa, 17% of phyla (2 of 12) and 38% of families (13
278 of 34) exhibited significant changes in relative abundance between the wet and dry seasons (**Fig.**
279 **2C**; **table S2**; linear models with false discovery rate (FDR) threshold = 0.05). These changes
280 were significant for the phyla Firmicutes and Tenericutes (**Fig. 2C, 2D**; **fig. S8**), and were
281 especially pronounced for the families Helicobacteraceae, Coriobacteriaceae, Burkholderaceae,
282 Bacteroidales RF16 group, vadinBE97, Spirochaetaceae, and Campylobacteraceae (**Fig. 2C**; **fig.**
283 **S9**). 28% of ASVs also exhibited significant changes in abundance across seasons (97 of 341
284 ASVs; linear models with FDR threshold = 0.05 for n = 393 models; **fig. S10**; **table S3**).
285 However, most gut microbial ASVs, families and phyla did not exhibit significant changes in

abundance across seasons, suggesting that many taxa play consistent roles in the gut throughout the year, including Kiritimatiellaeota, Elusomicrobia, Ruminococcacaceae, Clostridiaceae 1, and Rikenellaceae (**Fig. 2C**; **fig. S8, S9**; **table S2**).

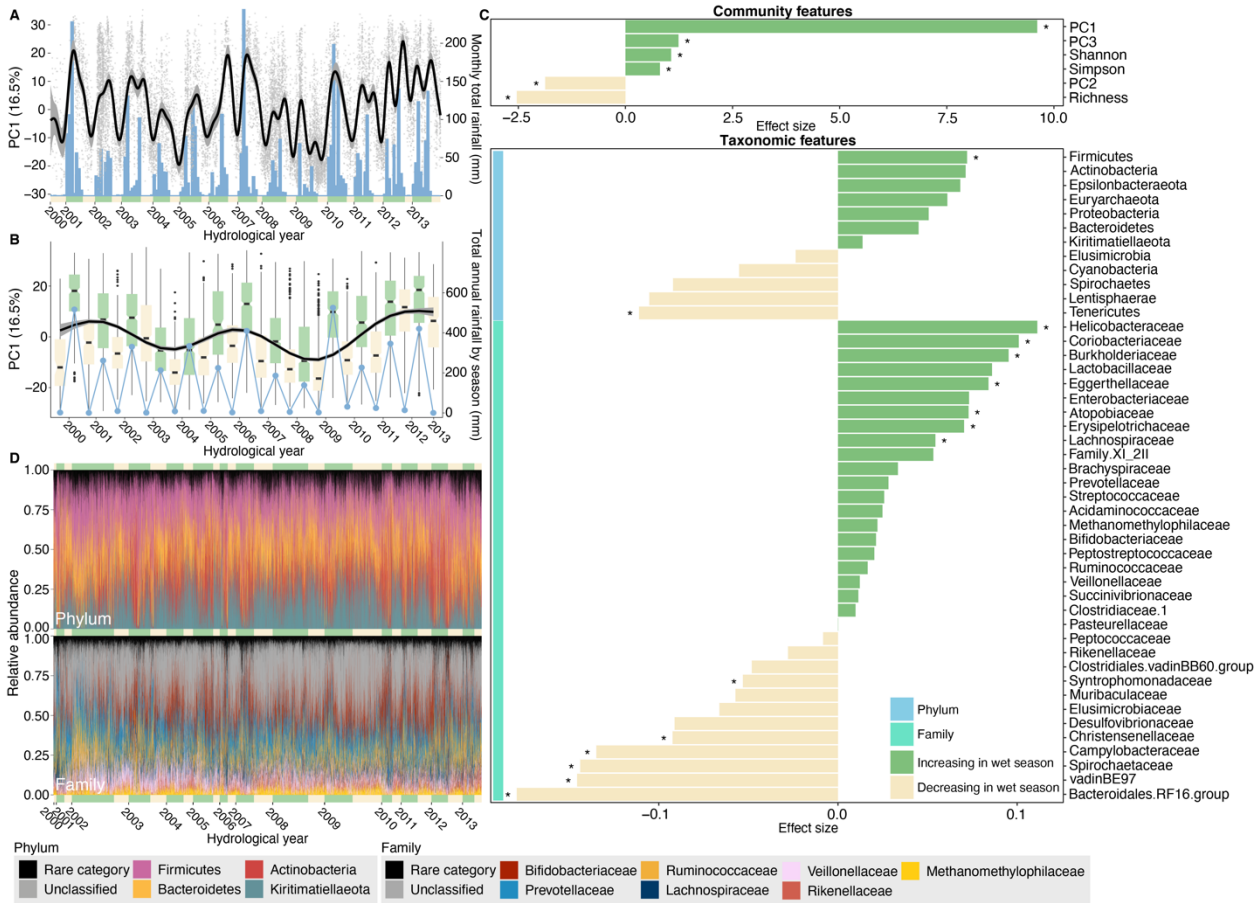

Fig. 2. Baboons show population-wide, cyclical shifts in microbiome community composition across seasons and years. (A) Changes in microbiome PC1 mirror monthly rainfall across all 14 years. The grey points show values of PC1 for each of the 17,265 samples (y-axis) on the dates they were collected (x-axis). The black line and its grey band show the predicted daily trend for PC1 across samples and its 95% simultaneous confidence interval, treating time as a continuous variable from April 21, 2000 to September 19, 2013. Blue bars show monthly rainfall (right-hand y-axis), and the yellow and green bars along the x-axis represent dry and wet seasons, respectively, with the width reflecting the number of months within the focal year with at least 1 mm rainfall. **(B)** Changes in microbiome PC1 on an annual scale across all 14 years (N = 17,265 samples). The box plots show the distribution of PC1 in wet (green) and dry (yellow) seasons. The black line shows the estimated annual trend for PC1 across all hydrological years, and the blue points show total annual rainfall (right-hand y-axis). **(C)** The effect of season varies across 52 features of the microbiome, including six community features (top panel) and 46 taxa (bottom panel; 12 phyla: light blue vertical bar; 34 families:

turquoise vertical bar; for 341 ASVs, see **fig. S13**). Each horizontal bar shows the effect of season from linear mixed models for each feature. Asterisks indicate features that changed significantly between the wet and dry seasons (N = 17,265 samples; FDR threshold = 0.05). See **figs. S8, S9** for feature-specific smooths and **fig. S10** and **table S3** for results for ASVs. **(D)** Bar plots showing the relative abundance of ASVs colored by four most common microbial phyla (above) and the seven most common families (below) across all 17,265 samples. Green and yellow bars along the x-axes represent wet and dry seasons, with the width corresponding to the number of samples in the focal hydrological year and season. 22.9% of ASVs (78 of 341) could not be assigned to a known family ("unclassified", shown in grey). The abundance of ASVs unclassified to family in the lower plot is ~35% because one unclassified ASV was the second most abundant ASV in the data set, with a mean abundance of 16.9% across all samples (ASV#2, phylum Kiritimatiellaeota, order WCHB1-41; **table S1**).

Baboon gut microbiota exhibit stronger idiosyncrasy than synchrony

While the microbiome metacommunity exhibited cyclical, seasonal shifts in composition, microbiome dynamics across different baboons were only weakly synchronized. Instead, consistent with prior observations of microbiome personalization[1, 20, 21, 22, 23, 24, 25], patterns of temporal autocorrelation indicated that each baboon exhibited largely individualized gut microbiome compositions and dynamics (**Fig. 3**). In support, ASV-level Aitchison similarity was much higher for samples collected from the same baboon within a few days of each other than for samples from different baboons over the same time span, regardless of whether those animals lived in the same or a different social group (**Fig 3A, 3B**; Kruskal-Wallis: $p < 2.2 \times 10^{-16}$ for all comparisons). Likewise, a PERMANOVA of Aitchison similarities between 4,277 samples from the 56 best-sampled hosts revealed that host identity explained 8.6% ($p < 0.001$) of the variation in community composition, much larger than sampling day or month (R^2 = 2.5% and 1.4%), group membership (2.2%), or the first three principal components of diet (0.04% to 2.4%; **table S4**; **fig. S11**).

Aitchison similarity among samples from the same baboon fell steeply for samples collected a few days to a few months apart, indicating that individualized dynamics are strongest for samples collected close in time (**Fig. 3A-3C).** At longer time scales (e.g., months and years), self-similarity was modest, but samples from the same baboon were significantly more similar to each other than they were to samples from different baboons, even for samples collected nearly three years apart (**Fig. 3A, 3C**; **fig. S12**). Following the initial steep decline in self-similarity, community similarity rose again slightly at 12-month intervals, both within and between hosts,

340 reflecting synchronized, seasonal microbial dynamics across the host population. These small,
341 12-month peaks in similarity were visible even for samples collected more than 5 years apart,
342 indicating that individual hosts and the population at large return to somewhat similar
343 microbiome community states on 12-month cycles over several years (**Fig. 3C**). Hence, the
344 patterns in **Fig. 3A** and **3C** show both idiosyncratic and synchronized microbial dynamics: over
345 short time scales, hosts are much more similar to themselves than they are to others, but on
346 annual scales, all hosts are weakly synchronized across seasons.

347 The greater influence of individualized dynamics compared to synchronized dynamics
348 can also be captured by comparing microbiome dynamics for deeply sampled hosts sharing the
349 same habitat at the same time (**Fig. 3D**; **fig. S13**). For instance, during the 2008-2009
350 hydrological year, we were able to collect nearly one sample per month from 17 individual
351 baboons. When we aligned these time series, we observed little evidence of shared changes in
352 the top three principal components of ASV-level microbiome composition across time, beyond
353 some overall seasonal patterns in PC1. We also observed little convergence to similar values
354 within any given month (**Fig. 3D**). Consequently, the microbiome of each baboon took a
355 different path over the ordination space over the same 1-year span (**fig. S13**). We found similar
356 results for another dense sampling period in the 2007-2008 hydrological year (**fig. S14**).

357 Microbiome taxa varied in their contributions to individualized gut microbiome
358 compositions (**Fig. 3E**; **fig. S15**). For example, for the 56 best-sampled hosts (**fig. S3**), several
359 phyla and families exhibited substantial variation in host mean clr-transformed abundance (i.e.,
360 across repeated samples for that host) compared to their mean clr-transformed abundance across
361 all hosts. These taxa included members of the phyla Cyanobacteria, Spirochaetes, Lentisphaerae,
362 and Elusimicrobia, and the families Spirochaetaceae, vadinBE97, Elusimicrobaceae, and
363 Muribaculaceae (**Fig. 3E**; **fig. S15**). These highly variable taxa tended to exhibit, on average,
364 below-average abundance compared to less variable taxa, which tended to exhibit, on average,
365 above-average abundance. Thus, idiosyncratic dynamics may be more often linked to uncommon
366 than common taxa, perhaps because uncommon taxa have greater functional variability across
367 hosts (**fig. S16**).

368 To test whether individualized gut microbiome compositions and dynamics could be
369 explained by microbial dispersal limitation between hosts, we used the Sloan Neutral

370 Community Model for Prokaryotes to estimate metacommunity-wide migration probabilities, *m*,
371 for ASVs in each season and hydrological year [45, 46]. As described above, *m* provides a measure
372 of dispersal limitation because it represents the probability that "vacancies" in a local community
373 (i.e. a host's microbiome) will be replaced by the process of dispersal from the microbiome
374 metacommunity (i.e. other hosts), as opposed to reproduction within a focal host's microbial
375 community [45, 46]. We found little evidence that dispersal limitation contributed to idiosyncratic
376 compositions and dynamics. The estimated probability that a given ASV lost from a host's
377 microbiota would be replaced by an ASV from another host in the population was nearly 40%
378 (the average host population-wide *m* across season and hydrological years = 0.373; range =
379 0.332 to 0.416; black points on **fig. S17**). These migration probabilities are generally lower than
380 those Sieber et al. [9] found for marine sponges sampled from the same coastal location (range of
381 *m* across sponge species: min=0.36; median=0.78; max=0.86) but much higher than for mice and
382 nematodes, both in natural and laboratory populations (mice: $m_{\text{wild}} = 0.11$ and $m_{\text{lab}} = 0.18$;
383 nematode: $m_{\text{wild}} = 0.03$ and $m_{\text{lab}} = 0.01$). Thus, they indicate that dispersal limitation is low for
384 baboon microbiota in Amboseli.

385 Interestingly, when we re-defined the microbiome metacommunity to be the host's social
386 group, instead of the whole host population, migration probabilities were similar (average *m*
387 across groups = 0.355; range = 0.347 to 0.365; colored points on **fig. S17**). Hence, despite
388 several studies that find microbiome compositional differences between hosts living in different
389 social groups, including in the Amboseli baboons[1, 41, 58, 59, 60, 61], social group membership does
390 not represent a major barrier to microbial colonization between baboons, perhaps because of
391 their overlapping home ranges, similar diets, and network connections via male dispersal (e.g.,
392 **Fig. 1**).

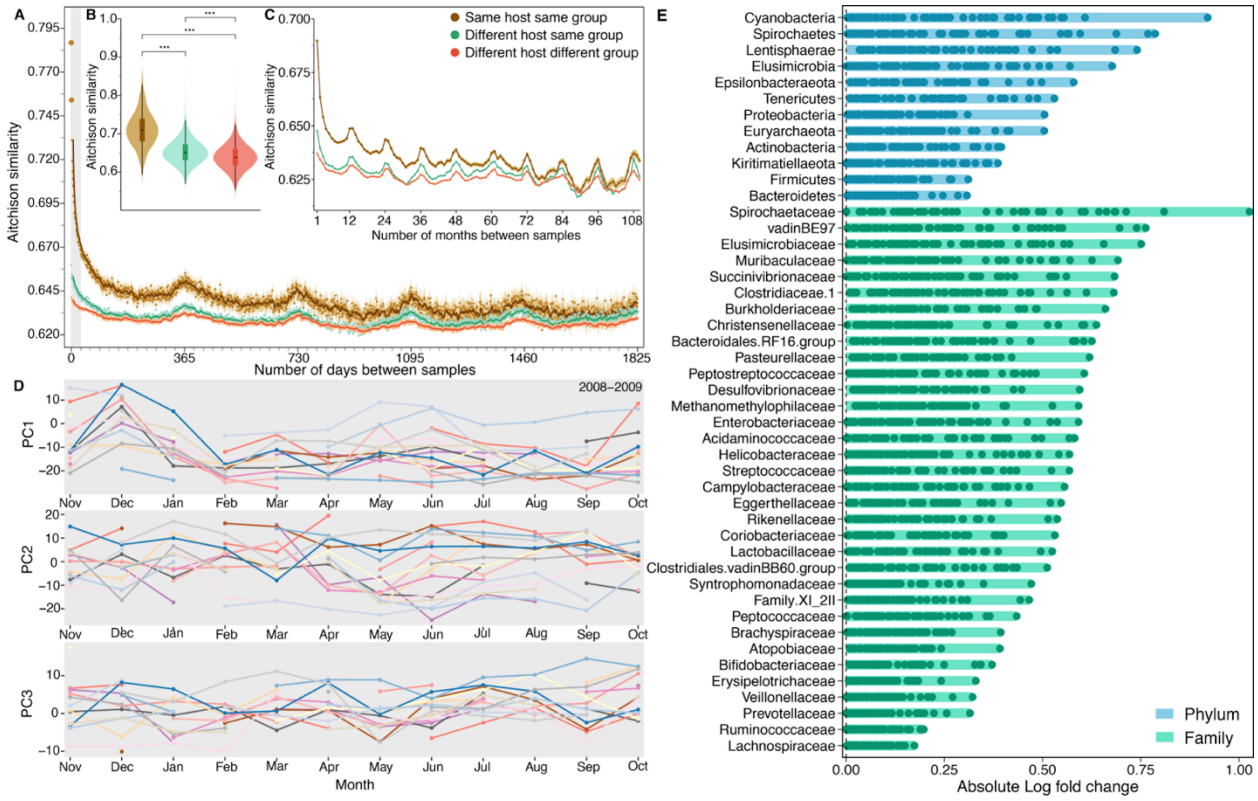

Fig. 3. Baboons exhibit largely idiosyncratic gut microbial compositions and dynamics. (A) Temporal autocorrelation in baboon gut microbiome communities for samples collected on the same day and up to 5-years (1,825 days) apart. Points show mean ASV-level Aitchison similarity (y-axis) between samples as a function of the number of days between sample collection (x-axis; small tick marks correspond to months). Lines depict moving averages (window size = 7 days). The grey region on the left indicates samples collected within one month of each other. Brown points show average Aitchison similarity between samples collected from the same baboon (N = 392,817 distinct sample pairs from 547 hosts with 2 or more samples); green points show similarity between samples from different baboons living in the same social group (N = 16,391,761 distinct sample pairs); orange points show similarity between samples from different baboons living in different social groups (N = 77,520,289 distinct sample pairs). **(B)** Average Aitchison similarity between pairs of samples collected within 10 days of each other. Samples from the same baboon are significantly more similar than samples collected from different baboons in the same or different social groups (Kruskal-Wallis; $p = 2.22 \times 10^{-16}$; N distinct sample pairs = 5,791 for within-host comparisons; 218,340 for different host same group; 779,054 for different host different group). **(C)** Temporal autocorrelation in Aitchison similarity on monthly scales for samples collected up to 10 years apart (N distinct sample pairs = 496,057 for within-host comparisons; 23,433,667 for different host same group; 114,170,919 for different host different group). **(D)** Microbiome dynamics for 174 samples from 17 baboons for which we had at least one sample from 10 or more months during the 2008-2009 hydrological year (Nov 2008 to Oct 2009). Panels show each individual's mean values for microbiome PC1, PC2, and

415 PC3; each colored line represents a distinct host. See **fig. S14** for similar results during another
416 densely sampled time period. Gaps indicate that the focal host did not have a sample in a given
417 month. **(E)** Some taxa have more idiosyncratic abundances than others. Each horizontal bar
418 shows a given taxon's minimum and maximum absolute log fold change in abundance across the
419 56 best-sampled hosts (hosts are represented as points within the bars; see **fig. S3** for information
420 on the 4,277 samples from the 56 best-sampled hosts). Absolute fold changes were calculated,
421 for a given taxon in a given host, as the taxon's average clr-transformed abundance across all
422 samples from that host, relative to the taxon's grand mean in all hosts in the population. Hosts
423 with large absolute fold changes for a given taxon therefore have abundances of that taxon that
424 are either well above or below-average compared to its abundance in the host population at large
425 (hosts with points close to zero exhibited taxonomic abundances typical of the population at
426 large). For many taxa, hosts varied in their absolute log ratio values, indicating that they also
427 deviated substantially from each other in the abundance of those taxa. Taxa (y-axis) are ordered
428 (from top to bottom) by their highest absolute log ratio value across the 56 best-sampled hosts.
429 Blue bars represent microbial phyla; green bars represent families. See **fig. S15** for a longitudinal
430 version of this analysis for the most and least idiosyncratic phyla and families.

431

432 **Shared environmental conditions are linked to modest synchrony across hosts**

433 To quantify the relative magnitude of idiosyncratic versus synchronized gut microbial
434 dynamics across the host population, social groups, and individual hosts, and to test whether
435 synchrony varies for a set of common microbial taxa, we used generalized additive models
436 (GAMs) to capture the nonlinear, longitudinal changes in 52 microbiome features (3 PCs of
437 ASV-level community variation, 3 metrics of ASV-level alpha diversity, and clr-transformed
438 relative abundances of 12 phyla and 34 families). For each feature, we ran three GAMs to
439 measure the deviance explained in gut microbial dynamics by successive sets of parameters,
440 reflecting the nested nature of our variables (**Fig. 4A**; x-axis of **Fig. 4C**; **table S5**). The
441 population-level model (i.e., model P) captured factors experienced by the whole host
442 population, including average rainfall and maximum daily temperature in the 30 days before
443 sample collection and random effect splines to capture monthly and annual cyclicity in
444 microbiome features (e.g., **Fig. 2A and B**; see **fig. S18** for effects of time of day, which was not
445 included in the model). The group-level model (i.e., model P+G) included all the predictor
446 variables in model P, and added a random effect spline for each social group, as well as variables
447 to capture temporal changes in each group's diet, home range use, and group size (**Fig. 4A, 4C**).
448 The host-level model (i.e., model P+G+H) included all of the predictor variables in model P+G,

and added a random effect spline for each host, and variables for host traits, including sex, age, and social dominance rank (**Fig. 4A, 4C**).

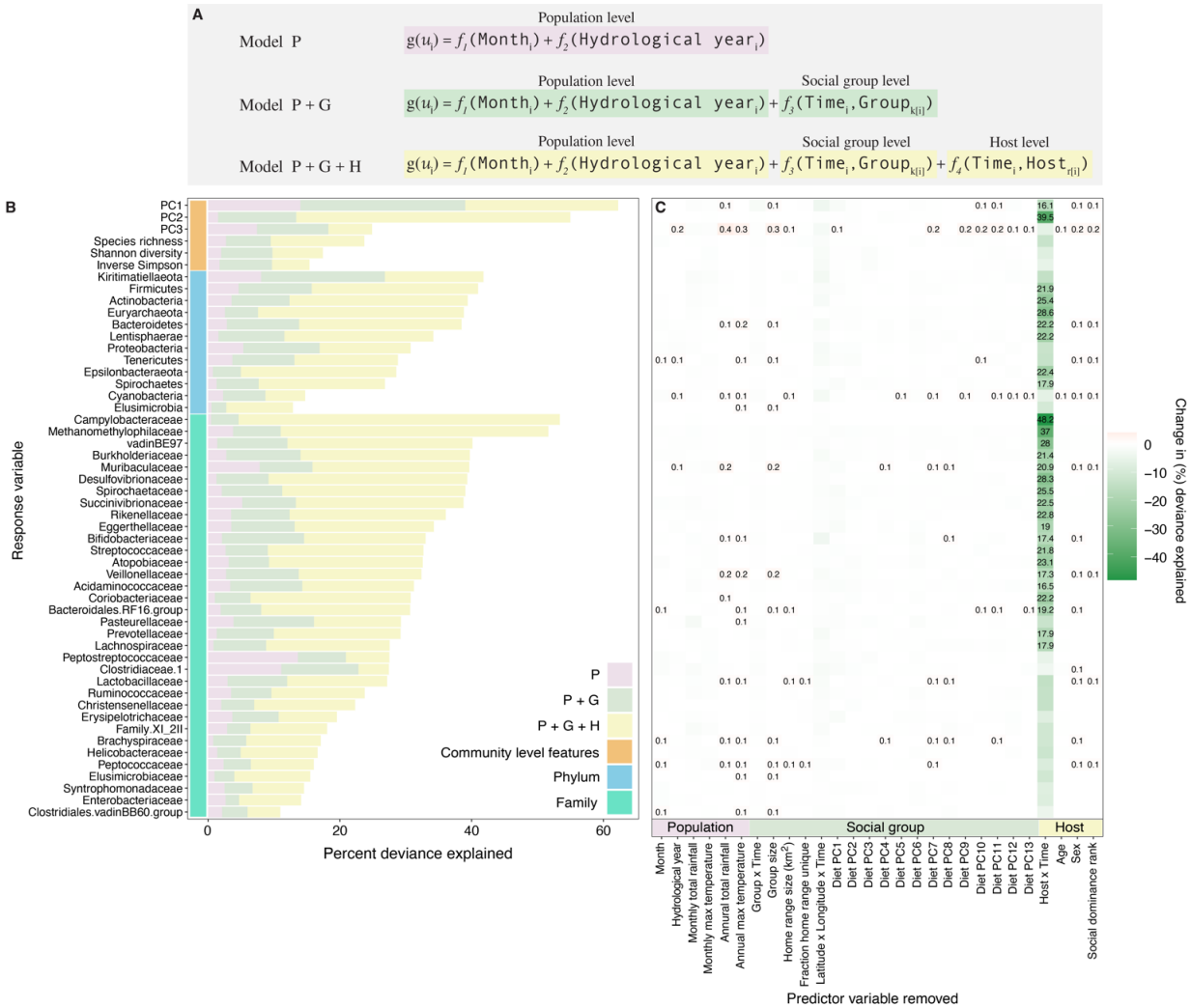

Fig. 4. Multilevel modeling identifies idiosyncratic microbial dynamics. (**A**) We fit three hierarchical GAMs to 52 microbiome features measured in 4,277 samples from the 56 best-sampled baboons, all of whom lived in the 5 social groups sampled the longest (between 2002 and 2010; median = 72.5 samples per host; minimum =48 samples; maximum = 164 samples; **fig. S3**). Each model contained successive sets of predictor variables reflecting population-level factors (pink), group-level factors (green) and host-level factors (yellow). The factors at each level are listed at the bottom of panel C and defined in **table S5**). Panel (**B**) shows, for each microbiome feature (i.e., response variable), the deviance explained by model P and the successive sets of predictor variables added in model P+G and model P+G+H, respectively (**table S6**; percent deviance is a measure of goodness-of-fit for nonlinear models and is analogous to the unadjusted R^2 for linear models). Panel (**C**) shows the loss in deviance explained for model P+G+H as we successively removed each predictor variable in turn from

464 model P+G+H, keeping the model otherwise intact (**table S7**). Losses in deviance are shown in
465 green, and we only provide numeric values for losses in deviance > 15%. Gains in deviance are
466 shown in red; we only show numeric values for gains > 0.1%.
467

468 Consistent with our autocorrelation analyses (**Fig. 3**), comparing the deviance explained
469 for each microbiome feature across the three models revealed stronger idiosyncratic than
470 synchronized dynamics for most microbiome features (**Fig. 4B, 4C**). Indeed, host-specific
471 factors, especially host identity, explained, on average, 10 times the deviance in the longitudinal
472 dynamics of microbiome features, compared to factors shared across hosts (i.e., group-level or
473 population-level factors). Specifically, model P only explained on average 3.3% (range = 0.46%
474 to 14.0%) of the deviance across all 52 microbiome features (pink bars in **Fig 4B**; **table S6**),
475 compared to 8.1% on average after adding group-level factors to the population-level model
476 (increase from model P to model P+G; range = 2% to 25%; green bars in **Fig. 4B**; **table S6**), and
477 30.1% of the deviance after including host-level dynamics (model P+G+H; range = 11.0% to
478 62.2%) for the same set of features (yellow bars in **Fig. 4B**; **table S6**). Importantly, the added
479 deviance for model P+G+H compared to model P or model P+G was not simply caused by
480 including more parameters. Specifically, randomizing host identity and host-level traits across
481 samples, while keeping each sample's annual, seasonal, and group identity intact, led to a
482 substantial drop in deviance explained compared to the real data (**fig. S19**). For instance, for
483 PC2, which was most strongly associated with host-level effects among all three PCs, the
484 deviance explained by model P+G+H dropped from 55% to 16.6% when host identity and traits
485 were randomized (**fig. S19;** see supplement and **fig. S20** for an additional analysis investigating
486 the effect of model complexity on deviance explained). That said, for PC3, randomized host-
487 level dynamics resulted in a 3% increase in deviance explained compared to the P+G model.
488 While less than the increase observed in the real data (6.6%), this result suggests that deviance
489 explained by the P+G+H model may be modestly inflated for some microbiome features.

490 44 of the 52 microbiome features exhibited greater gains in deviance explained by adding
491 host-level factors to model P+G, compared to adding group-level factors to model P. Of these 44,
492 22 features gained more than 20% deviance explained between model P+G and model P+G+H
493 (**Fig. 4B**; **table S6**). Three of the most common phyla, Actinobacteria, Bacteroidetes, and
494 Firmicutes all gained >20% deviance explained between model P+G and model P+G+H

495 (Actinobacteria = 27.1%; Bacteroidetes = 24.6%, and Firmicutes = 25.2%; **Fig. 4B**; **table S6**).
496 The most idiosyncratic features (i.e., those that gained >30% deviance explained by adding host-
497 level factors), were microbiome PC2, the phylum Euryarchaeota, and the families
498 Campylobacteraceae, Methanomethylophilaceae and Desulfovibrionaceae (**Fig. 4B**; **table S6**).
499 Notably, even the most synchronous feature, microbiome PC1 (14% deviance explained by the P
500 model), gained 23.2% deviance explained when adding host-level factors to the P+G model.

501 Removing covariates from model P+G+H one at a time, while keeping all other
502 covariates intact, revealed that host identity explained nearly all of the deviance in our models
503 (**Fig. 4C**; **table S6**; average loss in deviance explained by removing host identity = 17.3%
504 compared to 0.2% deviance for all other factors). Beyond host identity, the next most important
505 factor was the geographic area where the group traveled in the 30 days prior to sample
506 collection, which on average, explained 1% of the deviance across all 52 features, with the
507 strongest effects on microbiome PC1, Bifidobacteraceae, and Kiritimatiellaeota (**fig. S21**; **table**
508 **S6**). The removal of all other individual predictor variables had only minor effects on deviance
509 explained (**fig. S21**; **table S6**).

510 To investigate whether some of the idiosyncrasy we observed, especially at the host level,
511 was due to host genetic effects, we tested for a relationship between the deviance explained by
512 each GAM and the narrow-sense heritability (h^2) of microbiome taxon abundance as estimated
513 by Grieneisen et al.[33]. We found that higher levels of deviance explained by model P+G+H were
514 predicted by higher taxon heritability (Pearson correlation: R=0.37, p=0.016; **Fig. 5A**). In
515 contrast, we found no such effect at the population or group level, as expected since genotype is
516 a property of individual hosts, not groups or populations (model P+G: R=0.047, p=0.76; model
517 P: R=0.0085, p=0.96; **Fig. 5B**). In particular, we explained substantially more deviance by
518 adding the host level to model P+G for microbiome taxa with $h^2 > 0.05$ than we did for taxa with
519 very low h^2 values (model P+G+H: min=16.0, median=32.6, max=53.4 vs model P+G: min=4.6,
520 median=11.1, max=26.8; **Fig. 5B**). These results suggest that some idiosyncrasy in gut
521 microbiome dynamics is a consequence of differences in host genotype. However, because h^2
522 estimates from the animal model cannot be mapped directly onto estimates of deviance explained
523 in GAMs, direct estimates of genetic versus environmental effects on host dynamics remain an
524 important topic for future work.

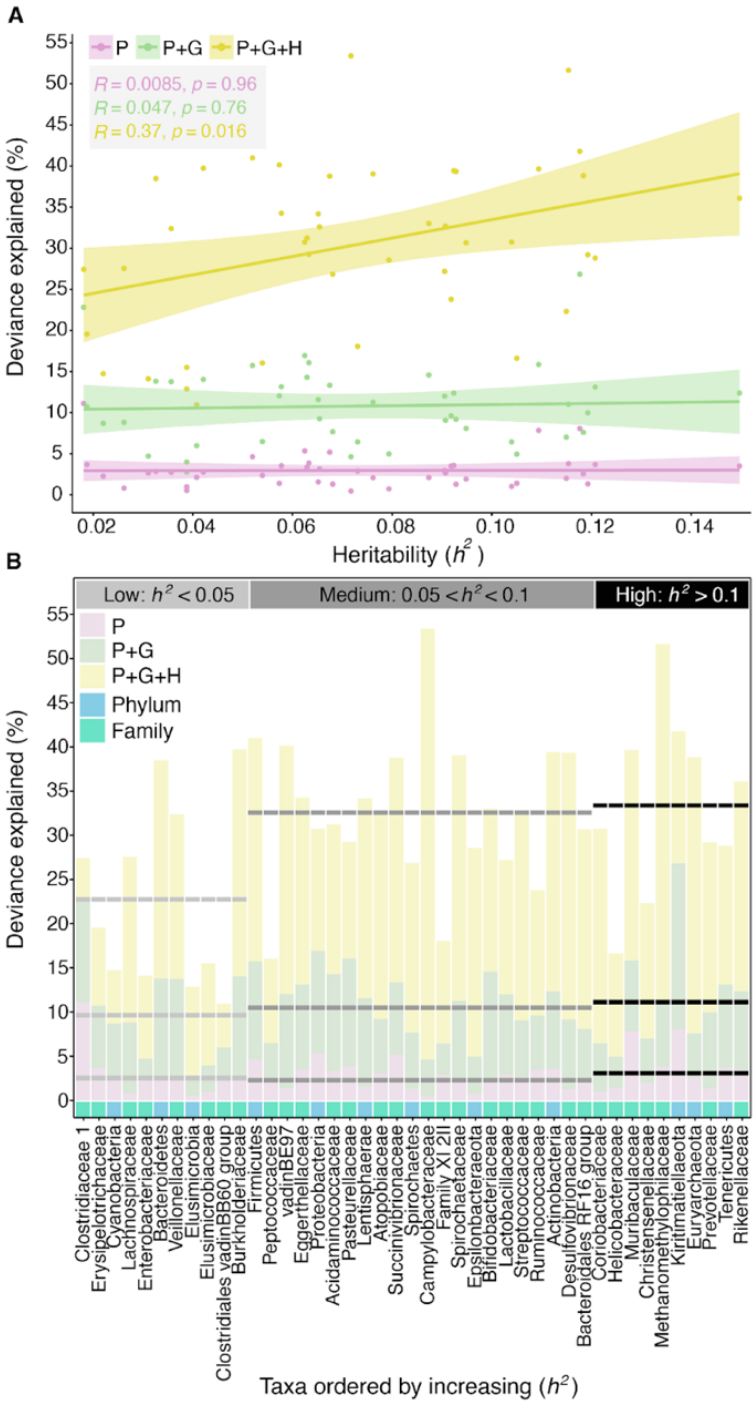

Fig. 5. Microbiome taxon heritability is associated with idiosyncratic dynamics. (**A**) Deviance explained (y-axis) by the phylum and family level GAMs (from **Fig. 4**) plotted against the focal taxon's heritability estimate (h^2; x-axis). Pink, green and yellow denote model P, model P+G and model P+G+H, respectively. (**B**) Deviance explained (y-axis) across the model hierarchy (pink: model P; green: model P+G; yellow: model P+G+H) for each taxonomic feature (i.e., at the phylum and family level; x-axis). The x-axis is ordered by increasing heritability with light blue and turquoise squares representing phyla and families, respectively. Horizontal dashed

533 lines show the average deviance explained per model for taxa with low heritability estimates (h^2
534 < 0.05; light gray); medium heritability estimates ($0.05 < h^2 < 0.1$; dark gray); and high
535 heritability estimates ($h^2 \geq 0.1$; black).

536

537 **Gut microbial dynamics among social group members are more synchronized than for the**
538 **host population at large**

539 Previous research in humans and other social mammals, including the Amboseli baboons,
540 finds that hosts in the same social group often have more similar gut microbiota than hosts in
541 different social groups e.g.[1, 41, 58, 59, 62]. Likewise, in our current data set, several taxa exhibited
542 abundances that were, on average, higher or lower within a given social group compared to their
543 average abundance in the host population at large (**fig. S22, S23**). Hence, we tested whether
544 shared social group membership is linked to greater microbiome community synchrony than
545 hosts in different groups. In support, the patterns of temporal autocorrelation in **Fig. 3A** showed
546 that hosts in the same group have detectably more similar microbiomes than those in different
547 groups, especially for samples collected within 10 days of each other (**Fig. 3B**; Kruskal-Wallis: p
548 $< 2.2\text{x}10^{-16}$). Likewise, samples from the same group tended to occupy similar ordination space
549 over time (**video S2**). While small, these group-level similarities were detectable, even for
550 samples collected more than 2 years apart (**Fig. 3C**; **fig. S12A**). The addition of group-level
551 splines to our GAMs led to gains in deviance that explained more than 10% for 15 of 52
552 microbiome features, including all three microbiome PCs, five phyla, and seven families (**Fig.**
553 **4B, 4C**; **table S6**). Several of these taxa were abundant in hosts, such as Firmicutes,
554 Bacteroidetes, and Bifidobacteriaceae (**Fig. 4B, 4C**; **table S6**).

555 Because each social group has a somewhat distinctive gut microbiota, the effects of
556 climate and diet on microbial dynamics may differ across groups. To test this idea, we added
557 interaction effects between group identity and climate variables (rain and temperature), or
558 between group identity and the first three PCs of diet to model P+G+H. However, these
559 interactions did not lead to substantial gains in deviance explained in our models (**fig. S24**; **table**
560 **S8**). For instance, adding the climate interactions explained on average an additional 0.95%
561 deviance across all 52 features (range = -1.9% to 5.4%; **table S8**), and diet interactions
562 explained, on average, an additional 1.2% deviance across all 52 features (range = -0.7% to
563 5.6%; **table S8**).

564 Gut microbial congruence among group members could also be linked to shared
565 behaviors and environments: baboons in the same group eat the same foods at the same time,
566 travel as a unit across the landscape, and may be grooming partners that are frequently in
567 physical contact (**Fig. 1B, 1D**; **video S1**;[33, 36, 37, 38, 39, 40]). Indeed, after host identity, the next most
568 important predictor variable in model P+G+H was the group's home range in the 30 days before
569 sample collection (**fig. S21**; **table S7**). Despite previous evidence for increased similarity in
570 microbiome profiles among grooming partners in the Amboseli baboons[41], we did not find
571 evidence for this pattern in our current data set (**fig. S25**). Samples collected within 30 days of
572 each other from individuals with strong grooming bonds were not substantially more similar than
573 samples from animals with weak or no observed grooming relationship (mean Aitchison
574 similarity between pairs with strong bonds = 0.645; mean Aitchison similarity between pairs
575 weak or no bond = 0.646; **fig. S26**). Because of differences in methodology, the lack of a
576 grooming effect in this data set should be interpreted with caution. Our prior research on this
577 topic[41] characterized microbial communities using shotgun metagenomic sequencing from >90%
578 of social network members, all within 30 days of each other. In contrast, this current data set
579 relies on 16S rRNA gene sequencing data from sparsely-sampled networks. Shotgun
580 metagenomic data provide much higher taxonomic resolution than 16S rRNA identities, and may
581 therefore more accurately capture the direct transmission between hosts.

582

583 **Conclusions**

584 Using an unusually large time series dataset from a population of wild baboons, we found
585 that gut microbial dynamics are both weakly synchronized across hosts and strongly
586 idiosyncratic to individual hosts. Like members of a poorly coordinated microbial orchestra,
587 microbial communities in different baboons are only weakly "in concert" across the host
588 population. Instead, consistent with prior studies in humans and some wild animals e.g.,[1, 20, 21, 22,
589 23, 24, 25], gut microbial dynamics are idiosyncratic at the level of individual hosts, and each
590 baboon "player" approaches the gut microbial "song" differently. Our results contribute to
591 mounting evidence that forces proposed to synchronize gut microbial metacommunities—shared
592 environments, diets, and high rates of between-host microbial dispersal—can create modest
593 synchrony among hosts, especially for hosts living in the same social unit. However, these forces

594 are typically not strong enough to overwhelm powerful and well-known drivers of microbiome
595 personalization, including host genetic effects, individual-level priority effects, horizontal gene
596 transfer, and functional redundancy[16, 17, 18, 19]. Interestingly, these idiosyncratic dynamics were
597 strong even for microbial phyla and families, whose dynamics reflect multiple microbial
598 functions and interactions that potentially buffer them against large fluctuations in abundance.
599 We expect that the personalized dynamics we observed will be even stronger for finer taxonomic
600 levels, especially bacterial species or strains that exhibit a high degree of functional variability
601 across hosts. In support, idiosyncratic dynamics were strongest for uncommon phyla or families
602 (**fig. S16**), which might exhibit greater functional variation across hosts than common, abundant
603 taxa.

604 Understanding the degree to which hosts in the same social group or population exhibit
605 shared versus idiosyncratic gut microbiome dynamics may be useful to researchers interested in
606 predicting individual microbiome changes, linking microbiome dynamics to health outcomes,
607 and designing broadly effective microbiome interventions. These objectives have already been
608 difficult to achieve, in part because of gut microbial personalization in humans and animals. For
609 instance, predictive models of gut microbiome dynamics from one person have been shown to
610 fail when they are applied to other people[27]. Although our focus here is on a single population of
611 baboons, limiting extrapolation to other species and populations, our results provide important
612 first-line evidence that microbiome predictions and interventions focused on microbiome taxa
613 may require approaches that are either personalized or focus on microbial function, as opposed to
614 taxonomic identities. Even then, "universal" microbiome therapies that work the same way for
615 all hosts may be unattainable. Instead, microbiome interventions will likely work best when they
616 are designed for host groups or populations that have shared compositions and dynamics.
617 Functional redundancy and horizontal gene flow may also mean that functions will be more
618 predictable than taxa, and prediction and intervention efforts that focus on microbiome
619 functional traits (e.g., metabolite levels; the presence of specific functional pathways) will likely
620 be less affected by gut microbiome personalization. Together, our results provide novel insights
621 about the extent and ecological causes of microbiome personalization, and they indicate that
622 personalized compositions and dynamics are not an artifact of modern human lifestyles and
623 environments.

624

Acknowledgments:

We thank Jeanne Altmann for her essential role in stewarding the Amboseli Baboon Project, and in collecting and maintaining the fecal samples used in this manuscript. We also especially thank the members of the Maasai pastoralist communities in the Amboseli-Longido areas, on whose land we have lived and worked for 50 years. We also thank the Kenya Wildlife Service, Kenya's Wildlife Research & Training Institute, the National Council for Science, Technology, and Innovation, and the National Environment Management Authority for permission to conduct research and collect biological samples in Kenya. We also thank the University of Nairobi, Institute of Primate Research, National Museums of Kenya, the Enduimet Wildlife Management Area, Ker & Downey Safaris, Air Kenya, and Safarilink for their cooperation and assistance in the field. We thank Karl Pinc for managing and designing the database. We also thank Tawni Voyles, Anne Dumaine, Yingying Zhang, Meghana Rao, Tauras Vilgalys, Amanda Lea, Noah Snyder-Mackler, Paul Durst, Jay Zussman, Garrett Chavez, and Reena Debray for contributing to fecal sample processing. Complete acknowledgments for the ABRP can be found online at https://amboselibaboons.nd.edu/acknowledgements/.

Funding: This work was supported by the National Science Foundation and the National Institutes of Health, especially NSF Rules of Life Award DEB 1840223 (EAA, JAG), and the National Institute on Aging R21 AG055777 (EAA, RB) and NIH R01 AG053330 (EAA), and NIH R35 GM128716 (RB), the Duke University Population Research Institute P2C-HD065563 (pilot to JT), the University of Notre Dame's Eck Institute for Global Health (EAA), and the Notre Dame Environmental Change Initiative (EAA). Since 2000, long-term data collection in Amboseli has been supported by NSF and NIH, including IOS 1456832 (SCA), IOS 1053461 (EAA), DEB 1405308 (JT), IOS 0919200 (SCA), DEB 0846286 (SCA), DEB 0846532 (SCA), IBN 0322781 (SCA), IBN 0322613 (SCA), BCS 0323553 (SCA), BCS 0323596 (SCA), P01AG031719 (SCA), R21AG049936 (JT, SCA), R03AG045459 (JT, SCA), R01AG034513 (SCA), R01HD088558 (JT), and P30AG024361 (SCA). We also thank Duke University, Princeton University, the University of Notre Dame, the Chicago Zoological Society, the Max Planck Institute for Demographic Research, the L.S.B. Leakey Foundation and the National Geographic Society for support at various times over the years.

Author contributions: EAA, JRB, LBB, RB, JAG, SM, and JT designed the research; EAA, SCA, RB, MRD, LG, JG, LRG, NG, SM, VY, NHL, TLW, RSM, JKW, LS, LBB, and JT, produced the data; JRB, TJG, DAWAMJ, LG, JCG performed the bioinformatics; JRB, KR, SM, performed the statistical analyses. EAA and JRB wrote the manuscript with important contributions from all authors.

Competing interests: The authors declare no competing interests.

Data and materials availability: 16S rRNA gene sequences are deposited on EBI-ENA (project ERP119849) and Qiita [study 12949, [63]]. Analyzed data and code is available on the first author's Open Science Framework / GitHub repository; for peer-review purposes, this is an anonymized link: https://osf.io/erdxa/?view_only=3323f05a5a9b479bac1124a5b07a62a9 .

References

1. Kolodny O*, et al.* Coordinated change at the colony level in fruit bat fur microbiomes through time. *Nature Ecology & Evolution* **3**, 116-124 (2019).

2. Schlomann BH, Parthasarathy R. Timescales of gut microbiome dynamics. *Curr Opin Microbiol* **50**, 56-63 (2019).

3. Koch H, Schmid-Hempel P. Socially transmitted gut microbiota protect bumble bees against an intestinal parasite. *Proceedings of the National Academy of Sciences* **108**, 19288-19292 (2011).

4. Finnicum CT*, et al.* Cohabitation is associated with a greater resemblance in gut microbiota which can impact cardiometabolic and inflammatory risk. *BMC Microbiology* **19**, 230 (2019).

5. Bashan A*, et al.* Universality of human microbial dynamics. *Nature* **534**, 259-262 (2016).

6. Costello EK, Stagaman K, Dethlefsen L, Bohannan BJ, Relman DA. The application of ecological theory toward an understanding of the human microbiome. *Science* **336**, 1255-1262 (2012).

7. Miller ET, Svanback R, Bohannan BJ. Microbiomes as metacommunities: understanding host-associated microbes through metacommunity ecology. *Trends in Ecology & Evolution*, (2018).

8. Bjork J, Díez-Vives C, Astudillo-García C, Archie EA, Montoya JM. Vertical transmission of sponge microbiota is inconsistent and unfaithful. *Nature Ecology & Evolution* **3**, 1172-1183 (2019).

9. Sieber M*, et al.* Neutrality in the Metaorganism. *PLoS Biol* **17**, e3000298 (2019).

10. Tredennick AT, dr Mazancourt C, Loreau M, Adler PB. Environmental responses, not species interactions, determine synchrony of dominant species in semiarid grasslands. *Ecology* **98**, 971-981 (2017).

11. Loreau M, de Mazancourt C. Species synchrony and its drivers: neutral and nonneutral community dynamics in fluctuating environments. *American Naturalist* **172**, E48-66 (2008).

12. Isbell FI, Polley HW, Wilsey BJ. Biodiversity, productivity and the temporal stability of productivity: patterns and processes. *Ecol Lett* **12**, 443–451 (2009).

13. Hector A*, et al.* General stabilizing effects of plant diversity on grassland productivity through population asynchrony and overyielding. *Ecology* **91**, 2213–2220 (2010).

14. de Mazancourt C*, et al.* Predicting ecosystem stability from community composition and biodiversity. *Ecology Letters* **16**, 617-625 (2013).

15. Gross K*, et al.* Species richness and the temporal stability of biomass production: a new analysis of recent biodiversity experiments. *Am Nat* **183**, 1-12 (2014).

16. Louca S*, et al.* Function and functional redundancy in microbial systems. *Nat Ecol Evol* **2**, 936-943 (2018).

17. Rainey PB, Quistad SD. Toward a dynamical understanding of microbial communities. *Philos Trans R Soc Lond B Biol Sci* **375**, 20190248 (2020).

18. Martiny JB, Jones SE, Lennon JT, Martiny AC. Microbiomes in light of traits: A phylogenetic perspective. *Science* **350**, aac9323 (2015).

19. Debray R, Herbert RA, Jaffe AL, Crits-Christoph A, Power ME, Koskella B. Priority effects in microbiome assembly. *Nat Rev Microbiol* **20**, 109-121 (2022).

20. Risely A, Wilhelm K, Clutton-Brock T, Manser MB, Sommer S. Diurnal oscillations in gut bacterial load and composition eclipse seasonal and lifetime dynamics in wild meerkats. *Nat Commun* **12**, 6017 (2021).

21. Franzosa EA*, et al.* Identifying personal microbiomes using metagenomic codes. *Proceedings of the National Academy of Sciences* **112**, E2930-E2938 (2015).

22. Faith JJ*, et al.* The long-term stability of the human gut microbiota. *Science* **341**, 1237439 (2013).

23. Bik EM, *et al.* Marine mammals harbor unique microbiotas shaped by and yet distinct from the sea. *Nat Commun* **7**, 10516 (2016).

24. Caporaso JG, *et al.* Moving pictures of the human microbiome. *Genome Biology* **12**, R50 (2011).

25. Costello EK, Lauber CL, Hamady M, Fierer N, Gordon JI, Knight R. Bacterial community variation in human body habitats across space and time. *Science* **326**, 1694-1697 (2009).

26. Flores GE, *et al.* Temporal variability is a personalized feature of the human microbiome. *Genome Biology* **15**, 531 (2014).

27. Johnson AJ, *et al.* Daily Sampling Reveals Personalized Diet-Microbiome Associations in Humans. *Cell Host & Microbe* **25**, 789-802 (2019).

28. Smits SA, Marcobal A, Higginbottom S, Sonnenburg JL, Kashyap PC. Individualized Responses of Gut Microbiota to Dietary Intervention Modeled in Humanized Mice. *mSystems*, (2016).

29. Rothschild D, *et al.* Environment dominates over host genetics in shaping human gut microbiota. *Nature* **555**, 210-215 (2018).

30. Falony G, *et al.* Population-level analysis of gut microbiome variation. *Science* **352**, 560-564 (2016).

31. Zhernakova A, *et al.* Population-based metagenomics analysis reveals markers for gut microbiome composition and diversity. *Science* **352**, 565-569 (2016).

32. Alberts SC, Altmann J. The Amboseli Baboon Research Project: Themes of continuity and change. In: *Long-term field studies of primates* (eds Kappeler P, Watts DP). Springer Verlag (2012).

33. Grieneisen L, *et al.* Gut microbiome heritability is nearly universal but environmentally contingent. *Science* **373**, 181-186 (2021).

34. Ren T, Grieneisen L, Alberts SC, Archie EA, Wu M. Development, diet, and dynamism: longitudinal and cross-sectional predictors of gut microbial communities in wild baboons. *Environmental Microbiology* **18**, 1312-1325 (2016).

35. Grieneisen L, *et al.* Genes, geology, and germs: gut microbiota across a primate hybrid zone are explained by site soil properties, not host species. *Proceedings of the Royal Society* **286**, 20190431 (2019).

36. Silk JB. Activities and feeding behavior of free-ranging pregnant baboons. *International Journal of Primatology* **8**, 593-613 (1987).

37. Altmann SA. *Foraging for Survival: Yearling Baboons in Africa*. University of Chicago Press (1998).

38. Bronikowski AM, Altmann J. Foraging in a variable environment: Weather patterns and the behavioral ecology of baboons. *Behavioral Ecology and Sociobiology* **39**, 11-25 (1996).

39. Muruthi P, Altmann J, Altmann S. Resource base, parity and reproductive condition affect females' feeding time and nutrient intake within and between groups of a baboon population. *Oecologia* **87**, 467-472 (1991).

40. Shopland JM. Food quality, spatial deployment, and the intensity of feeding interference in yellow baboons (*Papio cynocephalus*). *Behav Ecol Sociobiol* **21**, 149–156 (1987).

41. Tung J*, et al.* Social networks predict gut microbiome composition in wild baboons. *eLife* **4**, e05224 (2015).

42. Morton JT*, et al.* Establishing microbial composition measurement standards with reference frames. *Nat Commun* **10**, 2719 (2019).

43. Gloor GB, Macklaim JM, Pawlowsky-Glahn V, Egozcue JJ. Microbiome datasets are compositional: and this is not optional. *Front Microbiol* **8**, 2224 (2017).

44. R Core Team R. R: A language and environment for statistical computing. (available at http://www.R-project.org/). In: *R Foundation for Statistical Computing*) (2020).

45. Sloan WT, Lunn M, Woodcock S, Head IM, Nee S, Curtis TP. Quantifying the roles of immigration and chance in shaping prokaryote community structure. *Environmental Microbiology* **8**, 732-740 (2006).

46. Sloan WT, Woodcock S, Lunn M, Head IM, Curtis TP. Modeling Taxa-Abundance Distributions in Microbial Communities using Environmental Sequence Data. *Microbial Ecology* **53**, 443-455 (2007).

47. Burns AR*, et al.* Contribution of neutral processes to the assembly of gut microbial communities in the zebrafish over host development. *ISME Journal* **10**, 655-664 (2016).

48. Sprockett D. tyRa: Build Models for Microbiome Data. GitHub repository (available at https://danielsprockett.github.io/tyRa/articles/tyRa.html). (2020).

49. Oksanen J*, et al.* vegan: Community Ecology Package. R package version 2.5-7. (2020).

50. Vieira-Silva S*, et al.* Species-function relationships shape ecological properties of the human gut microbiome. *Nature Microbiology* **1**, 16088 (2016).

51. Wood SN. Stable and Efficient Multiple Smoothing Parameter Estimation for Generalized Additive Models. *Journal of the American Statistical Association* **99**, 673-686 (2004).

52. Wood SN. Fast stable restricted maximum likelihood and marginal likelihood estimation of semiparametric generalized linear models. *Journal of the Royal Statistical Society: Series B (Statistical Methodology)* **73**, 3–36 (2011).

53. Wood SN. *Generalized Additive Models: An Introduction with R, Second Edition* CRC Press (2017).

54. Hicks AL*, et al.* Gut microbiomes of wild great apes fluctuate seasonally in response to diet. *Nat Commun* **9**, 1786 (2018).

55. Orkin JD, Campos FA, Myers MS, Cheves Hernandez SE, Guadamuz A, Melin AD. Seasonality of the gut microbiota of free-ranging white-faced capuchins in a tropical dry forest. *ISME J* **13**, 183-196 (2019).

56. Baniel A*, et al.* Seasonal shifts in the gut microbiome indicate plastic responses to diet in wild geladas. *Microbiome* **9**, 26 (2021).

57. Mellard JP, Audoye P, Loreau M. Seasonal patterns in species diversity across biomes. *Ecology* **100**, e02627 (2019).

58. Moeller AH, Foerster S, Wilson ML, Pusey AE, Hahn BH, Ochman H. Social behavior shapes the chimpanzee pan-microbiome. *Science Advances* **2**, e1500997 (2016).

59. Lax S*, et al.* Longitudinal analysis of microbial interaction between humans and the indoor environment. *Science* **345**, 1048-1052 (2014).

60. Amato KR*, et al.* Patterns in gut microbiota similarity associated with degree of sociality among sex classes of a neotropical primate. *Microbial Ecology* **74**, 250-258 (2017).

61. Amato KR*, et al.* The role of gut microbes in satisfying the nutritional demands of adult and juvenile wild, black howler monkeys (*Alouatta pigra*). *American Journal of Physical Anthropology* **155**, 652–664 (2014).

62. Perofsky AC, Leriw RJ, Abondano LA, Di Fiore A, Meyers LA. Hierarchical social networks shape gut microbial composition in wild Verreaux's sifaka. *Proceedings of the Royal Society* **284**, 20172274 (2017).

63. Gonzalez A*, et al.* Qiita: rapid, web-enabled microbiome meta-analysis. *Nat Methods* **15**, 796-798 (2018).